**Atmospheric
Chemistry
and Physics**

Seasonal and diurnal variations of Hg° over New England

H. Mao, R. W. Talbot, J. M. Sigler, B. C. Sive, and J. D. Hegarty

Institute for the Study of Earth, Oceans and Space, Climate Change Research Center, University of New Hampshire, Durham, NH 03824, USA

Abstract. Factors influencing diurnal to interannual variability in Hg° over New England were investigated using multi-year measurements conducted by AIRMAP at the Thompson Farm (TF) coastal site, an inland elevated site at Pac Monadnock (PM), and two month measurements on Appledore Island (AI) in the Gulf of Maine. Mixing ratios of Hg° at TF showed distinct seasonality with maxima in March and minima in October. Hg° at AI tracked the trend at TF but with higher minima, while at PM the diurnal and annual cycles were dampened. In winter, Hg° was correlated most strongly with CO and NO_y, indicative of anthropogenic emissions as their primary source. Our analysis indicates that Hg° had a regional background level of ∼160 fmol/mol in winter, a dry deposition velocity of ∼0.20 cm s^{-1} with a ∼16 day lifetime in the coastal boundary layer in summer. The influence of oceanic emissions on ambient Hg° levels was identified using the Hg°-$CHBr_3$ correlation at both TF and AI. Moreover, the lower Hg° levels and steeper decreasing warm season trend at TF (0.5–0.6 fmol/mol d^{-1}) compared to PM (0.2–0.3 fmol/mol d^{-1}) likely reflected the impact of marine halogen chemistry. Large interannual variability in warm season Hg° levels in 2004 versus 2005/2006 may be due to the role of precipitation patterns in influencing surface evasion of Hg°. In contrast, changes in wintertime maximum levels of Hg° were small compared to drastic reductions in CO, CO_2, NO_y, and SO_2 from 2004/2005 to 2006/2007. These trends could be explained by a homogeneous distribution of Hg° over North American in winter due to its long lifetime and/or rapid removal of reactive mercury from anthropogenic sources. We caution that during warmer winters, the Hg°-CO slope possibly reflects Hg° loss relative to changes in CO more than their emission ratio.

1 Introduction

Atmospheric mercury exists in diverse chemical forms comprised of gaseous elemental mercury (Hg°), reactive gaseous mercury (RGM=$HgCl_2$+$HgBr_2$+HgOBr+...), and particulate mercury (Hg^P). The composition of total atmospheric mercury (i.e. the fraction of Hg°, RGM, and Hg^P) in the continental atmosphere varies geographically due to different land surface types, chemical environments, and human influences.

Numerous studies have measured the ambient level of total gas-phase mercury (TGM=Hg°+RGM) and Hg° at locations world-wide. For example, in the marine atmosphere over the North Atlantic Hg° levels are ∼1.6 ng m^{-3} (Laurier and Mason, 2007), between 1.6 and 4.7 ng m^{-3} over the North Pacific (Laurier et al., 2003), and 0.4–11.2 ng m^{-3} over the Mediterranean Sea (Sprovieri et al., 2003). At rural and mountainous sites in the northeastern and southeastern US, typical levels are ∼1.6 ng m^{-3} (Sigler and Lee, 2006; Valente et al., 2007), while concentrations as high as 5.1 ng m^{-3} are present in urban areas such as in Seoul, South Korea (Kim et al., 2005). Valente et al. (2007) summarized RGM levels over the continent, with values ranging from 0.1% (0.003 ng m^{-3}) of TGM at Zeppelin, Norway (Berg and Aspmo, 2003) to ∼6% (0.163 ng m^{-3}) at Oak Ridge Reservation in Tennessee (Lindberg and Stratton, 1998). Thus, in most regions the concentration of TGM can be approximated as that of Hg°.

Temporal variability in ambient mercury levels reflects the net effect of chemical and physical sources and sinks. The diurnal cycle of atmospheric mercury exhibits varying characteristics at different geographical locations. For example, measurements from 1 January to 31 December 2003 in St. Anicet (Québec, Canada), a flat grassy rural area surrounded by farms and woods, showed a strong diurnal cycle of Hg° with significantly higher concentrations during day- and nighttime than in early morning (Poissant et al., 2005).

This was similar to diurnal cycles observed at other locations in Canada and elsewhere (Kellerhals et al., 2003; Kim et al., 2005), and possibly reflects nighttime depletion of TGM by surface deposition. Quite differently, Lee et al. (1998) reported a nighttime enhancement in mercury near a power plant in Harwell, UK, in all seasons which they ascribed to a buildup of emissions under the nocturnal inversion layer. In summary, quantifying diurnal variability in ambient mercury levels is the first step to understanding its regional budget.

In the global budget of mercury, emissions from natural processes comprise 2100 tons Hg° yr^{-1} compared to 2400 tons yr^{-1} from anthropogenic sources (Mason and Sheu, 2002). Removal of Hg° from the atmosphere is facilitated by photochemical transformation to RGM with subsequent wet and dry deposition of Hg°, RGM, and Hg^P with efficiencies dependent on the proximity of sources, the level of oxidants, precipitation patterns, and land cover (Schroeder and Munthe, 1998). Laboratory-based studies have suggested that Hg° is converted to RGM and Hg^P at varying rates through reactions with O_3, OH, NO_3, and halogen atoms and oxides (Lin et al., 2006). However, chemical loss of Hg° has not been critically evaluated in the context of regional budgets.

Dry depositional loss of atmospheric Hg° appears to be small based on a small number of nighttime flux measurements (Obrist et al., 2006). Based on these limited measurements, the dry deposition velocity (v_d) is commonly set to values ranging from 0.01 cm s^{-1} down to zero in models (e.g. Lee et al., 2001; Bergan et al., 1999; Xu et al., 1999; Lindberg et al., 1992; Pai et al., 1997). In the Community Multiscale Air Quality model, CMAQ-Hg, the dry deposition velocity varied over the range of 0.02–0.1 cm s^{-1} over the forest and coastal surface in the Northeast US during months of June–September (modeling domain and seasonal average: 0.01±0.02 cm s^{-1}) (Talbot et al., 2006). However, field data from Lindberg et al. (1998) places the deposition velocity at one order of magnitude higher. They suggested that the foliar uptake or dry deposition of gas phase Hg° exhibited both cuticular and stomatal pathways, resulting in dry deposition velocities of 1.3±1.8 cm s^{-1} to wet and 0.4±0.3 cm s^{-1} to dry forest canopies.

Long-term measurements with high-time resolution are essential for assessing the regional budget of atmospheric mercury. Ideally, a co-located suite of meteorological and chemical measurements could help identify important sources and sinks of atmospheric mercury. In this study we used multi-year continuous measurements of Hg° from an inland site, a coastal site, and one season of measurements from a marine site to assess regional sources and sinks of Hg° in New England. We also explored the possible impact of inter-annual variability in the large-scale mercury background level on the regional characteristics of Hg°.

2   Measurements and data

Long-term continuous measurements with highest resolution possible were conducted at three UNH AIRMAP (www.airmap.unh.edu) Observatory sites: Thompson Farm (43.11° N, 70.95° W, 24 m), Pac Monadnock (42.86° N, 71.88° W, 700 m), and Appledore Island (42.97° N, 70.62° W, 40 m). Detailed information on the measurements can be found in Mao and Talbot (2004a), Talbot et al. (2005), and Fischer et al. (2007). Since January 2004 at TF, approximately 100 different hydrocarbons, halocarbons, and alkyl nitrates have been measured on a daily basis at 16:00 UT. Specifically, the observations of Hg°, CO, CO_2, O_3, SO_2, NO and NO_y at TF were used in this study, whereas at PM only measurements of Hg° and CO were available. At both TF and AI hourly measurements of volatile organic compounds (VOCs) were conducted during the International Consortium for Atmospheric Research on Transport and Transformation (ICARTT) field campaign in summer 2004 (Fehsenfeld et al., 2006). Information concerning the instrumentation configuration and measurement details are provided in Sive et al. (2005) and Zhou et al. (2005).

The PM and TF sites are 185 and 25 km inland from the Atlantic Ocean respectively, while AI is 10 km offshore in the Gulf of Maine. The locations of the measurement sites form a unique west-east oriented transect with site surroundings composed of heavily forested, coastal, and marine boundary layer environments. Moreover, due to the remote central location of PM in New England and its 700 m elevation (i.e. above the nocturnal inversion and in the middle of the daytime boundary layer), the site is ideally located to determine regional trends in trace gases, including Hg°.

At each site ambient air is delivered to the instruments through a 10 cm OD PFA Teflon-coated aluminum manifold operated at 1500 standard liters per minute. The inlets to the manifolds are located 15 m above ground level at TF and PM, just above the surrounding canopy, while that at AI is located at the top of a WWII-era surveillance tower about 40 m above sea level. The data were obtained as one minute averages for CO, O_3, CO_2, SO_2, NO, and NO_y. These data were merged to the five minute time resolution of the Hg° measurement. All data are presented in Universal Time (UT) with local time corresponding to UT−5 h for non-daylight saving time intervals and UT−4 h when daylight saving was in effect (i.e. April–October).

Measurements of TGM began at TF on 1 November 2003 and 28 February 2005 at PM, whereas measurements were available at AI only for the period of 8 July–6 September 2005. At all three sites a Tekran model 2537A cold vapor atomic fluorescence spectrometer was used to measure Hg° with a 5-min time resolution and a limit of detection of 5–10 fmol/mol. A teflon filter was used to exclude aerosols. The system employed an internal permeation tube calibration (±5% reproducibility) that was verified every six months using syringe injection from the headspace

of a thermoelectrically cooled Hg° reservoir (Tekran model 2505). Standard additions of Hg° were done using the internal permeation source of the Tekran. The concentration of these standard additions was 2–3 times higher than ambient mixing ratios. Standard additions of Hg° were performed twice daily on ambient air during day and night to capture variations in temperature and specific humidity. In practice the amount of TGM measured over a several minute time interval essentially represents Hg° unless there is an unusually large amount of RGM present. In most environments, a few minute sampling resolution for RGM is too short to detect levels near the detection limit. Independent measurements of RGM with a Tekran model 1130 show that at all three AIRMAP sites during mid-day in summer 2007 the RGM/TGM percentage rarely exceeded 1% (Sigler et al., 2008[1]). Thus, our TGM data can be approximated to be Hg° at all three sampling sites, and as such we refer to it as Hg° in this paper. In addition, we report Hg° in fmol/mol, and note that at STP 1 ng m^{-3}=112 fmol/mol.

The precision of the Hg° measurements was assessed by sampling ambient air at ground level using three co-located 2537A instruments at TF. These instruments were inter-calibrated using syringe injection from a Tekran 2505 unit prior to the ambient air measurement periods. We found that two brand new instruments agreed within ±4–5%, but that when a one-year old instrument was included the average increased to ±8–10%. Based on these comparisons, it appears that a conservative estimate of the overall measurement precision is ±10%. The accuracy of the Hg° measurements should be around ±5% due to careful calibration with the headspace injections. Future work will include rigorously re-assessing the overall accuracy of the calibrations when gas-phase calibration standards are available from the US National Institute of Standards and Technology.

3 Seasonal and diurnal variation

Time series of 5-min averaged Hg° mixing ratios are displayed in Fig. 1 at TF, PM, and AI for the entire study period. Mixing ratios of Hg° at TF exhibited a distinct and recurring seasonality with an annual maximum in late winter–early spring and a minimum in early fall. This long-term variation was accompanied by precipitous day-to-day dips and peaks that were accentuated during warm seasons. For example, Hg° mixing ratios in early fall were as low as ∼50 fmol/mol compared to the highest levels exceeding 300 fmol/mol. In comparison, Hg° at the PM inland site exhibited much smaller diurnal-to-annual variations and much higher minimum values. At this site, the daily mixing ratio maximum rarely exceeded 250 fmol/mol while the minimum was typically ∼100 fmol/mol. A comparison of Hg° seasonal

[1]Sigler, J. M., Talbot, R. W., Mao, H., et al.: Gaseous elemental and reactive mercury in southern New Hampshire, J. Geophys. Res., in preparation, 2008.
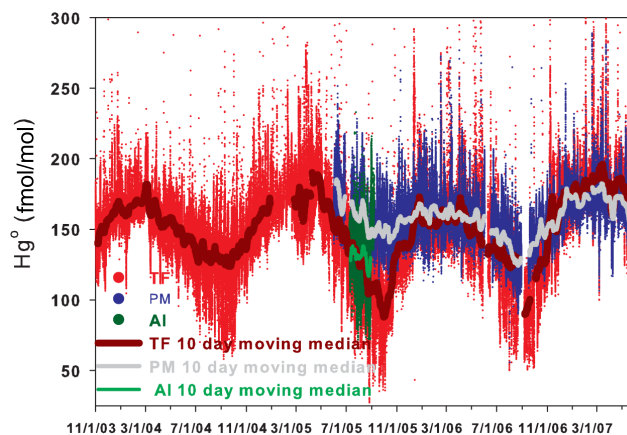

Fig. 1. Five-minute averaged mixing ratios of Hg° for TF (red) during the period of 1 November 2003 to 31 May 2007, for PM (blue) over 1 June 2005–31 May 2007, and for AI (green) over 8 July–6 September 2005. The smooth lines (TF – dark red, PM – grey, and AI – bright green) are 10-day moving medians.

statistics at the two sites is summarized in Table 1 with the sample size for each season. The 10th percentile, median and 90th percentile values of Hg° at TF were lower than those at PM by 10–50 fmol/mol in summer and fall, but were similar in winter and spring.

The annual maximum mixing ratios derived from the 10-day moving averages (Fig. 1, solid lines) were similar at both sites while the minimums were higher by 30–40 fmol/mol at PM. TF had a low annual maximum of 172 fmol/mol in 2006, a high of 190 fmol/mol in 2005 and 2007, and an intermediate of 182 fmol/mol in 2004. The highest annual minimum of 124 fmol/mol occurred in 2004 compared to only 88–90 fmol/mol in 2005 and 2006. Mixing ratios of Hg° rose rapidly from the minimum values in early November to the higher wintertime levels at rates of 0.75, 1.0, and 1.3 fmol/mol d^{-1} during 2004, 2005, and 2006, respectively, and hovered around these levels until early springtime. Note the sudden excursion at TF to an upward trend from the annual minimum, which apparently initiated the rapid increase in Hg° mixing ratios in fall. We attribute this to a sharp decline in both halogen chemistry impacts on Hg° and a decreased frequency of nocturnal inversions (Talbot et al., 2005). A similar trend occurs across New England for O$_3$, with the most extensive nighttime depletion occurring during the summer/fall months (Talbot et al., 2005).

The warm season (March–September) decline in Hg° at TF is seemingly indicative of a season-long strengthening in its removal processes, as evidenced by significant almost daily downward propagation in its mixing ratio. Over this time period Hg° decreased at 0.5–0.6 fmol/mol d^{-1} in all years except for 2004, when the rate was 0.3 fmol/mol d^{-1}. These rates of decrease were a factor of 2 smaller than the subsequent increase during the colder months. At PM
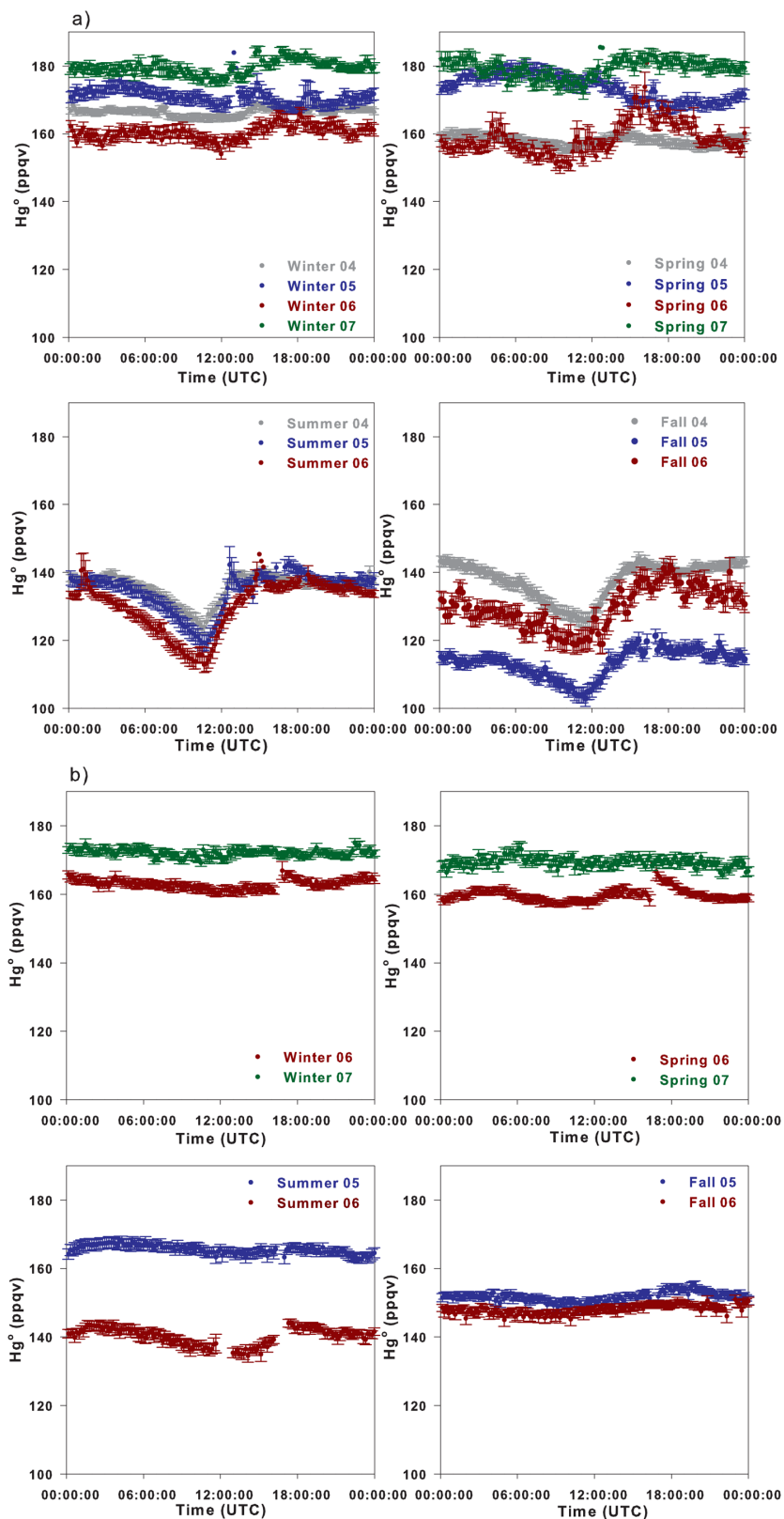
Fig. 2. Seasonally averaged diurnal cycles with standard deviation of means at TF **(a)** and PM **(b)**.

Table 1. Summary statistics (N – number of data points, 10th – the 10th percentile value, Med – the median value, 90th – the 90th percentile value, Mean – the mean value, σ – standard deviation. All measures are in unit of fmol/mol, except N) of Hg° mixing ratios at TF and PM for all seasons.

	TF					PM				
	N	10th	Med	90th	Mean $\pm\sigma$	N	10th	Med	90th	Mean $\pm\sigma$
04 Winter	24 069	154	166	179	167±12					
Spring	24 583	140	157	179	158±16					
Summer	24 541	114	136	156	136±17					
Fall	24 236	114	138	162	138±22					
05 Winter	13 771	153	168	192	177±22					
Spring	19 870	149	172	198	174±21					
Summer	25 079	103	136	161	134±26	20 822	145	163	189	166±18
Fall	22 367	85	112	143	113±23	25 498	136	151	169	152±15
06 Winter	18 528	142	156	185	160±19	23 277	147	161	181	163±15
Spring	18 132	136	156	182	159±27	22 767	146	158	174	160±13
Summer	16 178	109	131	150	130±22	20 177	121	140	159	141±28
Fall	18 712	89	127	171	130±32	18 701	133	148	164	148±14
07 Winter	18 510	163	178	194	179±16	17 351	159	171	186	172±12
Spring	18 441	153	179	202	179±23	18 564	150	169	187	169±16

the downward trend was much less pronounced, which may be attributable to the presence of a stronger natural source strength or less efficient loss of Hg°, assuming a similar regional anthropogenic contribution at the two sites.

Seasonally averaged diurnal cycles of Hg° at TF exhibited noticeable daily patterns in summer and fall with amplitudes of 20–25 fmol/mol and 15–20 fmol/mol respectively (Fig. 2a). The fluctuations were insignificant in winter and spring with amplitudes <10 fmol/mol. These seasonal characteristics are likely attributable to the presence and frequency of the occurrence of the nocturnal inversion at altitudes below ~300 m in New England (Talbot et al., 2005). During summer and fall the inversion can be present on as many as 50% of the nights, and like O₃, it inhibits near-surface replenishment of Hg° by limiting exchange with remnant boundary layer air aloft. Beneath the inversion, Hg° can be effectively removed from the atmosphere by nighttime sinks (e.g. oxidation and dry deposition), causing the observed nighttime dips in Hg° mixing ratios at TF (Fig. 2a). The daily minimum in Hg° mixing ratios occurred between 10:00–11:00 in summer and ~11:00 in fall, which correspond to sunrise and initiation of vertical mixing driven by diurnal heating (Talbot et al., 2005). We discuss this phenomenon in more detail in Sect. 5.

In contrast, predominant features at PM included the absence of an Hg° diurnal cycle and relatively small seasonal variation in its mixing ratio (160–175 fmol/mol) except for a moderate decrease to ~150 fmol/mol in falls 2005 and 2006 and a more significant one to ~140 fmol/mol in summer 2006. Comparison of Hg° seasonality at PM and TF indicates that mixing ratios at the two sites were similar in winter and spring, but lower at TF in summer and fall, with the

largest differences of 20–50 fmol/mol occurring near 12:00 in fall (Fig. 2a, b).

It should be pointed out that at TF there was considerable interannual variability (20–30 fmol/mol) in the seasonally averaged diurnal cycle of Hg° for all seasons but summer (Fig. 2a); this difference was most pronounced during the fall season. Furthermore, the patterns and magnitude of the interannual variability for spring, winter, and fall were different, which may reflect the dominance of varying controls on Hg° levels that potentially differ by season and year.

4 Relationship of Hg° with key trace gases

Both Hg° and CO have significant anthropogenic sources and exhibit similar annual cycles (Fig. 3). Thus, it can be insightful to examine the relationship between Hg° and CO. Annually, CO reached its lowest mixing ratios at TF (Fig. 3a) in June–July and remained low over the period July–October, followed by a maximum in mid-January to February. This is consistent with the annual cycle of OH, as variation in CO is driven primarily via oxidation by OH. In comparison, the timing of maxima and minima in Hg° lagged behind that of CO by 2–3 months. This implies that other equally or more important oxidative processes beside reaction with OH and/or possible sources influence the annual temporal variation of Hg°. It should be noted that annual cycles of Hg° and CO at PM resembled those at TF with less variability (Fig. 3b) due to its more rural and higher elevation location.

Identification of a positive correlation between a trace gas of interest and CO, a general tracer of combustion emissions, is an effective way to demonstrate the important contribution of anthropogenic sources to the atmospheric mixing ratio of
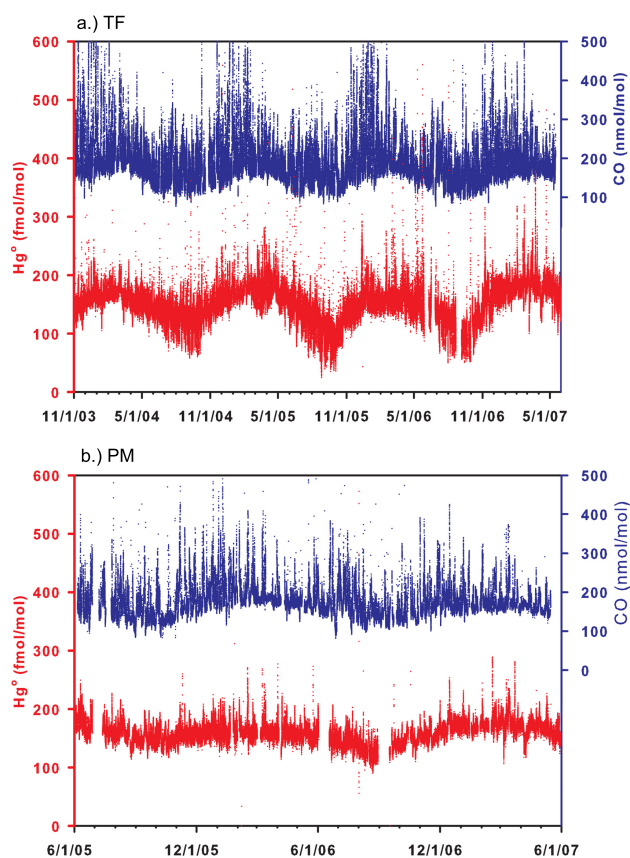
Fig. 3. Time series of 5-min averaged Hg° (red) and CO (blue) at TF **(a)** during the time period of 1 November 2003–31 May 2007 and at PM **(b)** over 1 June 2005–31 May 2007.

a trace gas (Parrish et al., 1993). To minimize confounding issues with natural sources of Hg°, we examined the wintertime relationship between Hg° and CO at TF and PM and found good linear correlations, indicating that the primary source of Hg° in winter at our sites was anthropogenic emissions. The 2006 Hg°-CO relationship at PM exhibited a relatively tight linear correlation with r^2=0.53 (p=0.01) and a slope of 0.23±0.003 fmol/nmol (p=0.05), while the correlation in winter 2007 yielded r^2=0.34 (p=0.01) and a slope of 0.21±0.006 fmol/nmol (p=0.05) (Fig. 4). In atmospheric mercury budgets, it is commonly assumed that the principal anthropogenic source of mercury is emissions from coal-fired power plants and waste incineration (Pacyna and Pacyna, 2002; Seigneur et al., 2004). A linear Hg°-CO relationship indicates that the two trace gases have long enough lifetimes to become well mixed in air masses on a regional scale. More specifically, their mixing ratios represent contributions of all anthropogenic emissions impacting the regional air shed superimposed on the background Hg° level. As mentioned in Sect. 2, the PM site is particularly well suited to determine the regional source characteristics of Hg°. Nonetheless, because PM is situated 1–3 transport days downwind of the polluted northeast corridor and the Mid-West, it is challenging to delineate the contribution from different sources to the ambient level of Hg° in New England.

Applying the Hg°-CO relationship, we deduced the regional background level of Hg° in air masses that affect New England. First, the lowest 10th percentile of CO mixing ratios were 164 nmol/mol and 154 nmol/mol at PM in winters 2006 and 2007 respectively, which we defined as the regional background level. The background levels of Hg° were then estimated to be 154 fmol/mol and 165 fmol/mol in winters 2006 and 2007 respectively, which are close to the seasonally averaged Hg° mixing ratios of 163 fmol/mol and 172 fmol/mol in winters 2006 and 2007 (Table 1).

A striking difference between the two sites was the factor of 2 lower slope values for Hg°-CO and Hg°-NO$_y$ at TF compared to PM. Interpretation of these relationships at TF is not straightforward owing to local sources and more variable transport to the site (Mao and Talbot, 2004b), with r^2 values for Hg°-CO ranging from 0.15 in 2005 to 0.31 in 2004 during the four winters (Fig. 5) (all with p=0.05 except 2005). Note that the slope values exhibited strong interannual variability, and increased by more than a factor of 2 from 0.06±0.001 fmol/nmol (p=0.05) in winter 2004 to 0.14±0.004 fmol/nmol (p=0.05) in winter 2006. Furthermore, the maximum mixing ratio of CO in winters 2006 and 2007 did not exceed 600 nmol/mol, whereas in winter 2003 CO peaked at close to 1000 nmol/mol. Lower maximum levels were also observed in CO$_2$ and NO$_y$ at TF in winters 2006 and 2007 compared to previous years, indicating that less polluted air masses arrived at the site. The Hg°-NO$_y$ relationship observed at TF in winter had large interannual variability in the slope values (Fig. 6). Similar to the Hg°-CO correlation, the slope value increased by more than a factor of 2 from 0.50±0.01 fmol/nmol (p=0.05) in winter 2004 to 1.22±0.02 fmol/nmol (p=0.05) in winter 2006. The mechanisms driving this phenomenon are explored in Sect. 7.2.

The relationships of Hg° with C$_2$Cl$_4$, C$_2$HCl$_3$, O$_3$, CO$_2$, SO$_2$, and CH$_4$ were investigated at TF. Our analysis showed that Hg° was not correlated with C$_2$Cl$_4$, C$_2$HCl$_3$, O$_3$, and SO$_2$ (not shown). It is reasonable not to observe relationships between Hg° and C$_2$Cl$_4$ as well as C$_2$HCl$_3$ due to their different sources and lifetimes. Gaseous elemental mercury is primarily emitted from combustion sources and has a lifetime of 0.5–2 years (Schroeder and Munthe, 1998), while C$_2$Cl$_4$ and C$_2$HCl$_3$, used as degreasing agents in industrial applications, have lifetimes of a couple of months (Kindler et al., 1995; Olaguer, 2002; NOAA GMD, 2000) and 4–7 days (Kindler et al., 1995), respectively.

Because the main source of SO$_2$ is coal-fired power plants, whose emissions may also contribute significantly to atmospheric mercury, it has been used as a mercury tracer in previous studies. For example, Friedli et al. (2004) found that Hg° was well correlated with CO and SO$_2$ in plumes sampled over the western North Pacific during the ACE-Asia airborne field campaign. However, our long-term data set at TF shows no obvious correlation between Hg° and SO$_2$
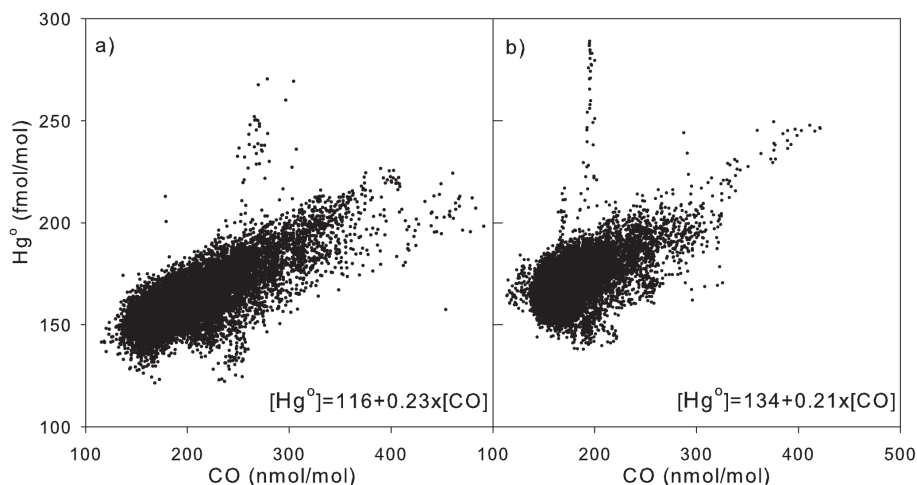
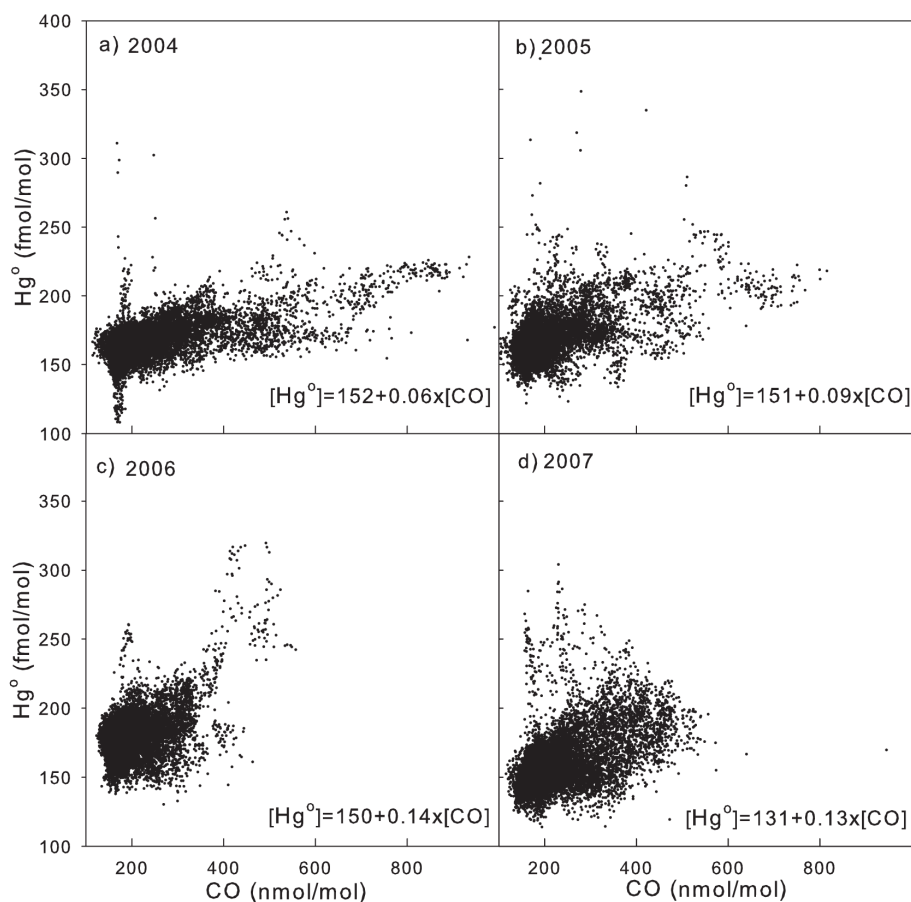**Fig. 4.** Five-minute averaged Hg° versus CO mixing ratios at PM in winters 2006 **(a)** and 2007 **(b)**.

Fig. 5. Five-minute averaged Hg° vs. CO mixing ratios at TF during winters 2004 **(a)**, 2005 **(b)**, 2006 **(c)**, and 2007 **(d)**.

in all seasons except winter when there was a diffuse positive correlation ($r^2 < 0.2$) in all four winters (2004–2007, not shown). This result most likely reflects the increased lifetime of SO_2 in winter, which persists over extended trans-

port times and retains the source signature longer than in the warm season. In all other seasons, the largest mixing ratios of SO_2 corresponded to low-to-moderate levels of Hg° (100–200 fmol/mol) with no identifiable relationship. Overall, TF
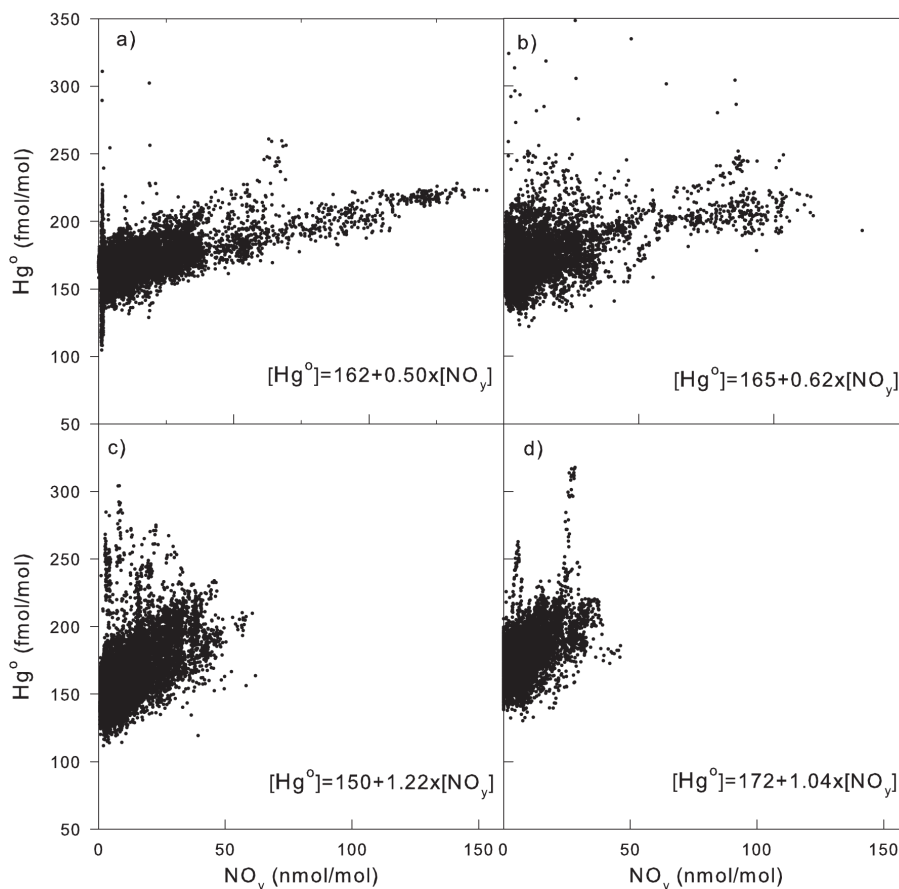
Fig. 6. Five-minute averaged Hg° vs. NO$_y$ mixing ratios at TF during winters 2004 **(a)**, 2005 **(b)**, 2006 **(c)**, and 2007 **(d)**.

may be too distant from significant coal-fired combustion sources in the eastern and midwestern US to define a consistent relationship between Hg° and SO$_2$.

There is an excellent positive linear correlation between greenhouse gases and combustion tracers in New England, indicating a significant anthropogenic impact on regional air quality (Shipham et al., 1998a, b). Since Hg° was correlated reasonably well with CO in winter, we examined its relationships with CO$_2$ and CH$_4$ during winter when natural source/sink strengths are minimal. As expected, the correlation between Hg° and CO$_2$ (not shown; r^2=0.3–0.5 , slope = 1.6–1.8 fmol/mmol) was similar to that of Hg°-CO. The correlation between Hg° and CH$_4$ was poor, likely related to weaker CH$_4$ emissions compared to CO$_2$ from combustion sources.

5 Nighttime depletion and dry depositional losses

Time series of O$_3$ and Hg° mixing ratios for August 2004, 2005, and 2006 show synchronized depletion in the early morning hours (Fig. 7). The nighttime dips in Hg° were most pronounced when the O$_3$ mixing ratio approached zero, presumably nights with strong nocturnal inversions. The oc-

currence of O$_3$ depletion results from titration by NO and dry deposition, combined with negligible vertical exchange with residual boundary layer air aloft (Talbot et al., 2005). In contrast, a continuous enhancement in CO$_2$ mixing ratios to 500–600 mmol/mol occurs until sunrise (not shown), driven by emissions from ecosystem respiration and local combustion processes (Talbot et al., 2005). The coincident depletion of Hg° and O$_3$, and enhancement in CO$_2$ provides strong evidence for a net surface sink of Hg°.

Sinks of Hg° are in general considered to be chemical oxidation and dry deposition. Total chemical loss of Hg° through reaction with O$_3$, OH, and NO$_3$ was estimated using typical mixing ratios at TF and published rate constants. These estimates were in very close agreement for the 2004 and 2005 warm seasons in spite of year-to-year differences in mixing ratios of Hg°. The reaction of Hg° with NO$_3$ can be a significant nighttime loss pathway for Hg° (Sommar et al., 1997). Using k_{NO3}=4×10^{-15} cm^3 molecule^{-1} s^{-1} (Sommar et al., 1997), a NO$_3$ mixing ratio = 10 pmol/mol (Brown et al., 2004; Ambrose et al., 2007) and Hg°=100 fmol/mol, the loss rate of Hg° would be 0.35 fmol/mol h^{-1} or 3.5 fmol/mol d^{-1} for 10 h of darkness.
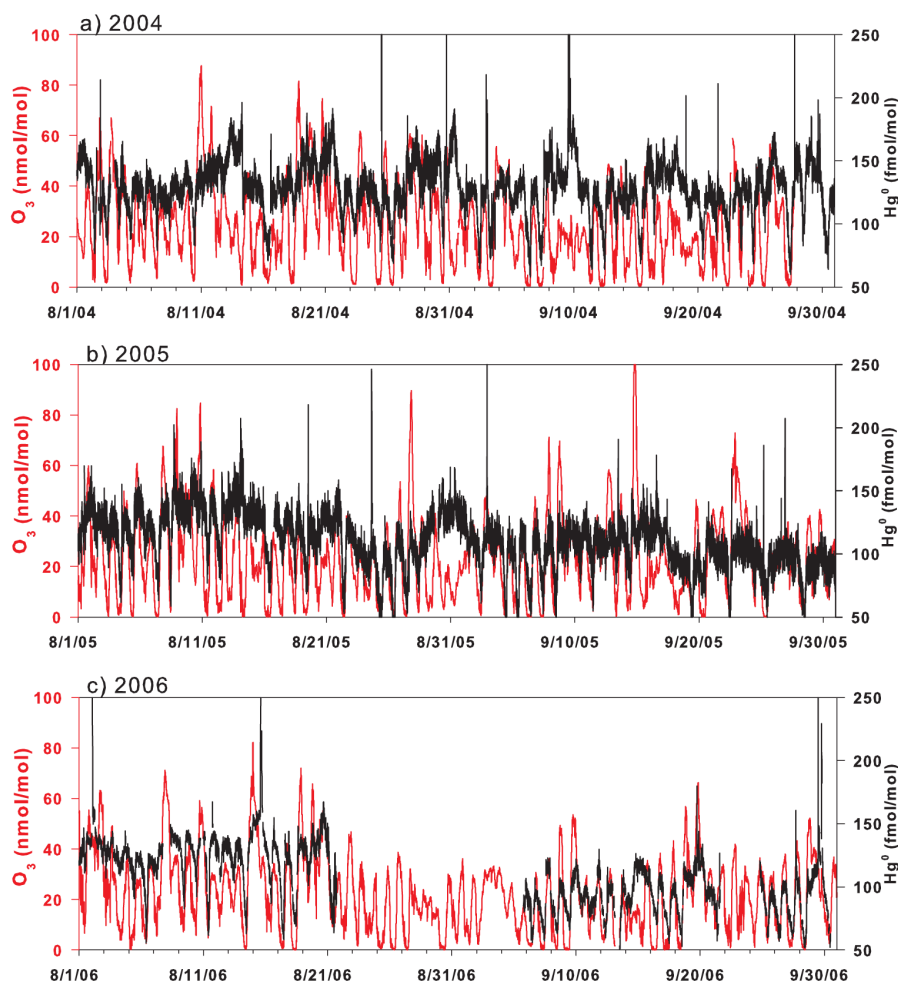
Fig. 7. Time series of 5-min averaged Hg° (black) and O$_3$ (red) during the time period of 1 August–30 September for 2004 **(a)**, 2005 **(b)**, and 2006 **(c)**.

Published rate constants for reaction of Hg° with O$_3$ vary greatly, yielding significantly different estimates of Hg° loss. The lower limit of the rate constant is 3×10^{-20} molecule^{-1} cm^3 s^{-1} (Hall, 1995), while the upper limit is 7.5×10^{-19} molecule^{-1} cm^3 s^{-1} (Calvert and Lindberg, 2005). The seasonally averaged loss rates from 2004, 2005, and 2006 were very similar, differing only by a few percent, and thus the averaged loss rates were listed in Table 2. Using the upper limit, total daily loss of Hg° during the 2004 warm season at TF varied from ~12 fmol/mol d^{-1} in April to ~5 fmol/mol d^{-1} in fall (Fig. 8a). Results are comparable for 2005 and 2006; to avoid redundancy only values for 2005 are shown in Fig. 8b. The estimated Hg° loss resulting from oxidation by OH (OH concentration adopted from Spivakovsky et al., 2000; rate constant from Sommar et al., 2001) was negligible compared to that of O$_3$. Note that on average, day- and nighttime total loss (O$_3$+OH+NO$_3$) (4.7 and 6.1 fmol/mol d^{-1}, respectively) were of equal importance, while loss of 2.6 fmol/mol d^{-1} by reaction with O$_3$

Table 2. Daytime, nighttime, and daily (daytime + nighttime) loss rates of Hg° (fmol/mol d^{-1}) at TF averaged over the warm seasons 2004, 2005, and 2006 via reactions with O$_3$ (O$_3^1$ – using rate constant of 7.5×10–19 cm^3 molecule^{-1} s^{-1}, O$_3^2$ – rate constant of 3.0×10^{-20} cm^3 molecule^{-1} s^{-1}). Total rates of loss are the summation of the day- and nighttime rates of loss via O$_3$, OH, and NO$_3$.

	Daytime	Night	Daily
O$_3^1$	4.2	2.6	6.8
O$_3^2$	0.2	0.1	0.3
OH	0.5	–	0.5
NO$_3$	–	3.5	3.5

at night was comparable to the 3.5 fmol/mol d^{-1} by NO$_3$ (Table 2).

Calvert and Lindberg (2005) cautioned that significant loss of Hg° by the Hg°-O$_3$ reaction is not likely to occur in the
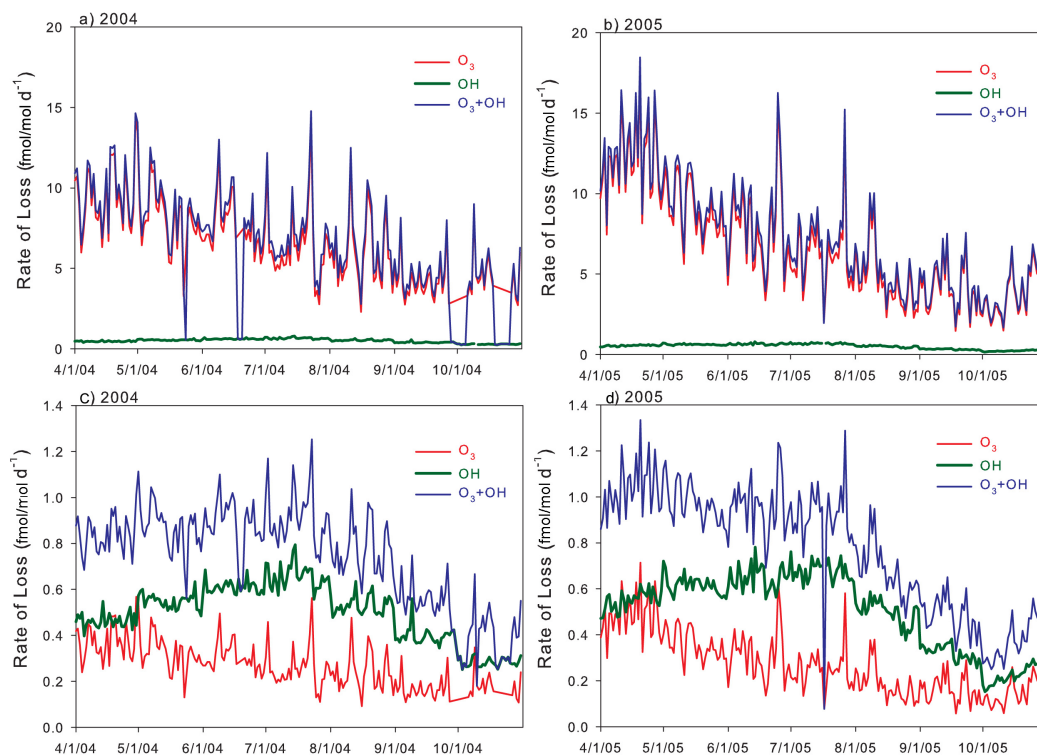
Fig. 8. Rate of loss of Hg° via oxidation reactions with O_3 (red), OH (green), and the total rate of loss during the warm season (1 April–31 October) in 2004 **(a, c)** and 2005 **(b, d)**. The largest reaction rate constant 7.5×10^{-19} cm^3 molecule^{-1} s^{-1} (Calvert and Lindberg, 2005) was used in (a) and (b), and a constant on the lower end 3.0×10^{-20} cm^3 molecule^{-1} s^{-1} (Hall, 1995) was used in (c) and (d).

atmosphere. Using the lower limit of the rate constant, we found that the Hg° loss via oxidation by O_3 was smaller than that via OH oxidation (0.3–0.7 fmol/mol d^{-1}), decreasing from 0.4 fmol/mol d^{-1} in April to 0.1 fmol/mol d^{-1} in fall (Fig. 8c–d). Overall, the total chemical loss of Hg° via oxidation by OH and O_3 ranged from $\sim$1 fmol/mol d^{-1} in April to 0.4 fmol/mol d^{-1} in fall. Table 2 shows that on average, the lower limit of daily total chemical loss (O_3+OH+NO_3) was 4.3 fmol/mol d^{-1}, and the nighttime loss via reaction with NO_3 comprised more than 80% of its removal.

The seasonally averaged diurnal cycles of Hg° in summer and fall showed $\sim$20 fmol/mol of nighttime Hg° loss (Fig. 2a). Dry deposition of Hg° has been treated as a minor loss mechanism in previous studies, but our observations and analysis suggest otherwise. To quantify the lower limit of dry depositional loss, we used the upper limit attributed to chemical loss using the fastest rate constant for the Hg°-O_3 reaction. Hence, nighttime chemical loss of Hg°, $\sim$6 fmol/mol d^{-1}, comprised 30% of the 20 fmol/mol seasonal average nighttime decrease (Fig. 2a).

We propose that removal by dry deposition was the main contributor to the remaining 70% of the nighttime loss of Hg°. The loss of Hg° via dry deposition can be better inferred from its relationship with NO_y, in particular, by inference to HNO_3 and NO_x. A scatter plot of Hg° versus NO_y (Fig. 9a),

using all 3.5 years of data from TF, exhibited a well-formed correlation envelope along the lower boundary of the relationship. This boundary was comprised of the lowest Hg° values and NO_y ranging from near zero to 140 nmol/mol (i.e. data colored red in Fig. 9a, denoted as lower Hg°-NO_y boundary hereinafter). The data points on this boundary for NO_y mixing ratios >40 nmol/mol were mostly collected in winter (December–February) and resided on the high end of NO_y distribution at TF (Fig. 6a and b). The data points on this boundary for NO_y <40 nmol/mol mostly occurred before sunrise in fall to early December (Fig. 9b), and exhibited a linear function that was represented by

$$Hg° = 48 + 3.2 \times NO_y. \tag{1}$$

Diurnal cycles of Hg°, NO_y, and O_3 were averaged over the 17, 44, and 24 days in 2004, 2005, and 2006, respectively, that included the data points for NO_y <40 nmol/mol on the lower Hg°-NO_y boundary (Fig. 10). On these days, O_3 mixing ratios decreased quickly from 15–20 nmol/mol at 00:00 to single digits in <4 h and subsequently decreased at a much slower rate to ≤5 nmol/mol in the hours preceding sunrise. NO_y and Hg° fell at more constant rates over the same time period, implying a common loss mechanism. The differing nighttime depletion rates of NO_y and Hg° from that of O_3 may stem from coexisting sources for NO_y and Hg°
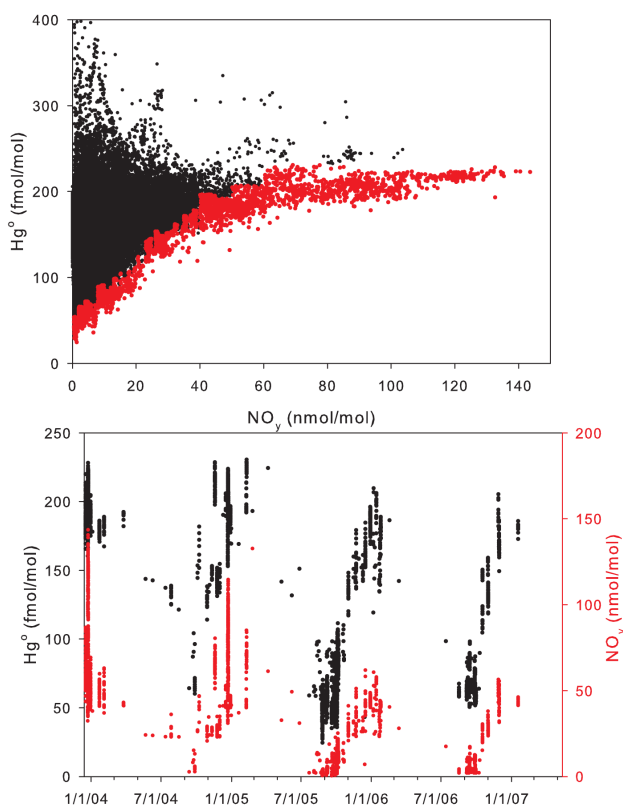
Fig. 9. (a) All data points of 5-min averaged Hg° vs. NO$_y$ over 1 November 2003–31 May 2007 with the lower boundary of the relationship highlighted in red ; **(b)** The time of occurrence of the data points that comprised the lower boundary in (a).

Fig. 10. Averaged diurnal cycles of Hg° (black), NO$_y$ (red), and O$_3$ (blue) for the days (17, 44, and 24 days in 2004, 2005, and 2006, respectively) that include the data points with NO$_y$<40 nmol/mol on the lower boundary of Hg° vs. NO$_y$ presented in Fig. 9a for 2004 **(a)**, 2005 **(b)**, and 2006 **(c)**.

as opposed to no nighttime O$_3$ production but loss from NO titration and dry deposition. Therefore, NO$_y$ appears to be a better proxy than O$_3$ to understand nighttime loss mechanisms of Hg°.

Nighttime loss of NO$_y$ is mainly via the dry deposition of HNO$_3$ and NO$_x$. Nighttime loss of HNO$_3$ is on average ∼1 nmol/mol in this area based on ICARTT measurements during summer 2004 (Fischer et al., 2006). An additional 5 nmol/mol of NO$_x$ is lost at night through interconversion of NO$_x$-NO$_3$-N$_2$O$_5$ and ultimate removal of N$_2$O$_5$ based on measurement and model findings for the ICARTT period (Ambrose et al., 2007). As a result, dry depositional loss of (HNO$_3$+NO$_x$) is fast at night, and thus the close resemblance of decreasing nighttime trends of NO$_y$ and Hg° equates to more rapid dry deposition of Hg° than suggested in previous studies. Using the slope of 3.2 fmol/nmol derived in Eq. (1) and 6 nmol/mol loss of NO$_y$ we obtained ∼20 fmol/mol loss of Hg° at night via dry deposition. This is nearly identical to the ∼20 fmol/mol seasonal average value suggested in Fig. 2a, which represents the combined result of anthropogenic sources and removal processes (oxidation and dry deposition) at night.
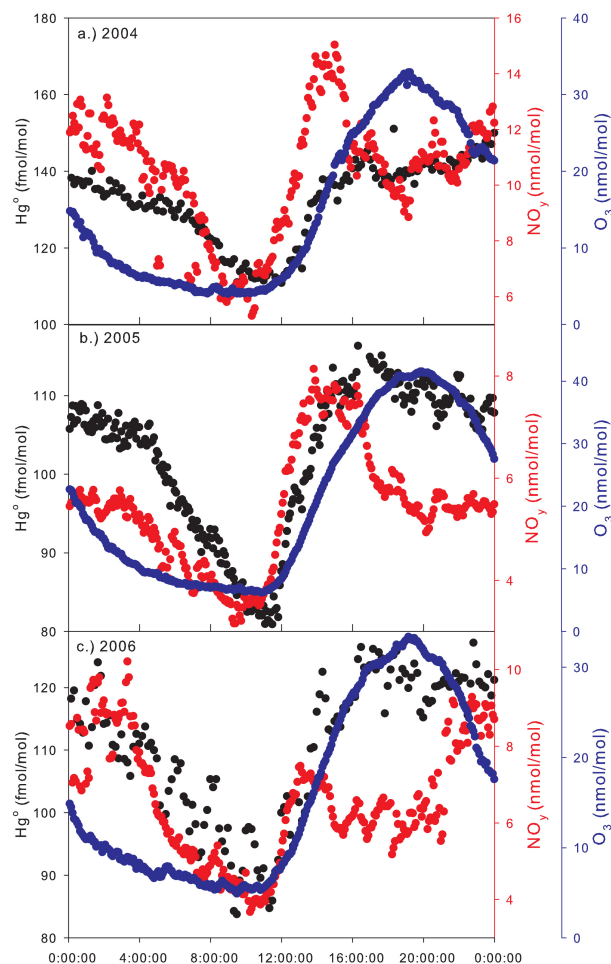
However, we estimate a total average Hg° daily loss (oxidation + deposition) of ∼26 fmol/mol, suggesting a source of ∼6 fmol/mol, likely from local anthropogenic emissions. The total annual emission of mercury in Strafford County, NH (1000 km^2), where TF is located, is ∼6850 g yr^{-1} (NESCAUM, 2005a, b), which yields ∼9 fmol/mol assuming a nocturnal inversion layer thickness of 125 m (Talbot et al., 2005). This is of similar magnitude as the ∼6 fmol/mol source needed to close the budget.

To minimize the source and sink terms in the budget calculation, we consider nights with the occurrence of a nocturnal inversion layer, where the nighttime decrease in Hg° is determined by the net effect of chemical loss, dry deposition, and anthropogenic sources. Using a surface depletion zone of 125 m (Talbot et al., 2005), we found that the dry deposition velocity of Hg° was 0.17 cm s^{-1} in 2004, 0.20 cm s^{-1} in
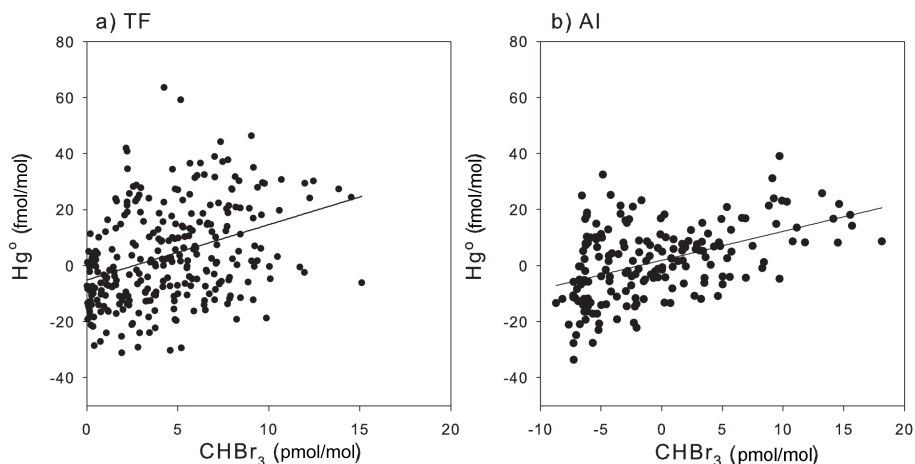
Fig. 11. Anomalies of Hg° versus CHBr$_3$ at TF (**a**) during summers 2004 and 2005 and at AI (**b**) in summer 2005. Anomalies were calculated by subtracting the hourly averages for the entire campaign period from the measured high resolution mixing ratios.

2005, and 0.18 cm s^{-1} in 2006. These values represent nighttime deposition rates, and, similar to O$_3$ at a forested site in central Massachusetts (Munger et al., 1998), are likely increased during daytime due to open plant stomata and higher wind speeds.

An estimate of the warm season Hg° lifetime was made using the formula from Jacob (1999). Based on v_d=0.2 cm s^{-1}, an average Hg° mixing ratio of 150 fmol/mol, a seasonally averaged chemical loss rate of 0.5 fmol/mol d^{-1} (using the lower limit), and a planetary boundary layer (PBL) height=2000 m, we obtain an atmospheric lifetime of ∼16 days. The lifetime estimated here is an order of magnitude smaller compared to 160 days for v_d=0.01 cm s^{-1}, a commonly used value in regional and global models. Our analysis indicates that deposition processes for Hg° are in fact very significant, and the lifetime of Hg° in the local planetary boundary layer at TF is short.

6 Oceanic influence

In Sect. 3 we showed that the rate of decrease in Hg° mixing ratios during the warm season was typically 0.5–0.6 fmol/mol d^{-1} at TF compared to 0.2–0.3 fmol/mol d^{-1} at PM, which resulted in a cumulative difference of 55 fmol/mol between the two sites over the period 1 April to 30 September. Global budget estimates for Hg° indicate that the ocean is its largest natural source (Mason and Sheu, 2002) and is also a large reservoir of organo-halogen trace gases. This raises the possibility of an important oceanic influence on the ambient level of Hg° at TF, both as a direct source of Hg° and enhancement of Hg° lost from oxidation by halogen atoms and oxides.

Instantaneous variability in the ambient level of Hg° can be obscured if the magnitude of the change is small compared to the ambient mixing ratio and the impact is short-lived (i.e.

the measurement resolution of tracer compounds is not sufficient to capture the events). Moreover, TF is surrounded by extensive vegetation, located near the ocean, as well as being downwind of anthropogenic sources in the favorable southwest flow regime, resulting in complex and well-mixed contributions from a multitude of natural and anthropogenic sources. Consequently, clear correlations between the mixing ratios of Hg° and marine tracers (e.g. CHBr$_3$, CH$_2$Br$_2$, and CH$_2$ClI) were rarely observed in the overall dataset.

To accentuate the instantaneous variation, we defined "anomalies", which were calculated for Hg° and three marine tracers, CHBr$_3$, CH$_2$Br$_2$, and CH$_2$ClI by subtracting the diurnal and seasonal means from the measured mixing ratios over the entire ICARTT period (1 July–16 August 2004). The means can be considered to be the baseline for the time period of interest that is determined by processes operating on time scales of days or longer. The anomaly, in essence, represents the effects of instantaneous events such as in situ chemical oxidation, emissions, and dry deposition.

Using the criteria of CO<200 nmol/mol to eliminate direct anthropogenic influences, a time window of 1600–1800 for maximum onshore transport (Miller et al., 2003), and CHBr$_3$ anomalies >0 pmol/mol to capture the possible impact of oceanic emissions, we obtained a subset of 322 data points, or 25% of the 1314 data points for the entire period. A positive correlation, albeit diffuse, was identified between the Hg° and CHBr$_3$ anomalies with r^2=0.11 and a slope of 2.0 fmol/pmol (Fig. 11a). The correlation of Hg° anomalies with those of CH$_2$Br$_2$ and CH$_2$ClI also appeared to be positive to some extent but weaker possibly due to their much different lifetimes from that of Hg°. These results raised the possibility of an oceanic influence on the summertime ambient levels of Hg° at TF.

Measurements of Hg° were available at our marine site AI during the time period of July–August 2005, when there

were concurrent hourly VOC data. The data from the time window of 02:00–09:00 was selected when oxidation of Hg° by halogen compounds should be minimal, and consequently the effect of oceanic emissions should be apparent. Again, the criterion of CO<200 nmol/mol was applied to minimize the impact of anthropogenic sources. A positive correlation between the anomalies of Hg° and CHBr$_3$ was found to be better defined (r^2=0.21) (Fig. 11b) than at TF (r^2=0.11). This finding illustrates the oceanic source of Hg° in the marine boundary layer (MBL) and supports its potential influence on adjacent coastal areas such as at TF.

Oceanic emissions of organo-halogen species can cause loss of Hg° through oxidation reactions, such as with bromine (Br) atoms as described by Holmes et al. (2006). These mechanisms facilitate conversion of Hg° to RGM with subsequent rapid depositional loss as observed in the Arctic (Ariya et al., 2004). In the MBL with [Br]=0.5 pmol/mol (Dickerson et al., 1999), [Hg°]=100 pmol/mol, and k=3.2×10^{-12} cm^3 molecule^{-1} s^{-1} (Ariya et al., 2002), the production rate of RGM should be ∼14 fmol/mol h^{-1}. However, the reported concentrations of RGM in coastal and oceanic regions range from 6±6 pg m^{-3} (0.8 fmol/mol) in the North Pacific (Laurier et al., 2003) to 50±43 pg m^{-3} (6 fmol/mol) in Bermuda (Sheu, 2001). Our measurements at AI indicate an average RGM concentration of ∼100 pg m^{-3} (10 fmol/mol) over the Gulf of Maine in summer 2007 (Sigler et al., 2008[1]). The disparity between the estimated production rate and measured concentrations suggests that highly efficient RGM loss pathways exist in the MBL.

TF, being only 25 km away from the ocean, is under marine influence year-round, and is impacted by air masses directly from the ocean 30% of the time in summer (Chen et al., 2007). Thus, the potential loss of Hg° via halogen chemistry cannot be ignored in the regional budget of Hg°. We hypothesize that the overall significantly lower Hg° levels and steeper decreasing trend in Hg° mixing ratios during the warm season at TF compared to those at PM reflects an important impact of halogen chemistry on Hg°.

7 Contrasting interannual variability in Hg° between warm and cold seasons

7.1 Warm season

As shown in Sect. 3, Hg° mixing ratios at TF decreased progressively during the warm season. The magnitude of this decrease was similar during the warm seasons in 2005 and 2006 at a rate of 0.6 fmol/mol d^{-1}, steeper than the rate of 0.3 fmol/mol d^{-1} in 2004 (Fig. 12). Therefore, in this section, we focus on the change from 2004 to 2005 to identify possible causal mechanisms.

We proposed in Sect. 5 that dry deposition was the principal mechanism leading to decreased nighttime mixing ratios of Hg°. However, our calculations indicated that the
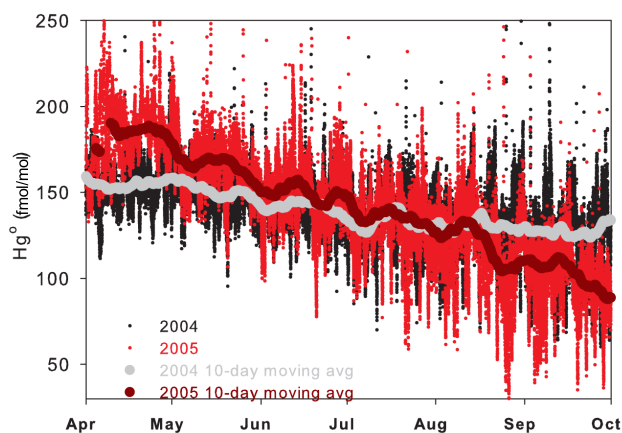

Fig. 12. Five-minute averaged Hg° mixing ratios at TF during the warm seasons in 2004 (black) and 2005 (red) with their respective 10-day running medians (2004 – grey and 2005 – dark red).

downward seasonal trend can not be attributed to dry depositional loss of Hg°, based on the little difference in depositional loss between the two years in spite of more frequent occurrences of nighttime Hg° depletion in 2005. To identify possible causes, we conducted a spectral analysis of the Hg° data over the time period April–September in 2004 and 2005. In both years the dominant periodicity was the diurnal cycle. However, >70% of the total energy was distributed over time scales of 2–30 days. Furthermore, we applied the Kolmogorov-Zurbenko (KZ) filter (Zurbenko, 1986; Hogrefe et al., 2000) to separate the diurnal (<1 day), synoptic (weekly), and long-term (>weekly) time scales. This revealed that in 2005, processes on time scales >weekly contributed 71% to the total variance compared to 32% in 2004. Thus, long-term processes might account for the more pronounced decreasing trend in 2005.

Processes on time scales >weekly can include chemical loss of Hg° through reactions with O$_3$ and OH, which are slower than ones with organo-halogen compounds, and variations in natural emissions which are influenced by climate. Our calculations revealed no distinct difference in seasonal trends in chemical oxidation by O$_3$ and OH during the two warm seasons (Fig. 10). Hydrocarbon measurements at TF from the two years showed similar levels of marine-derived halogenated trace gases such as CHBr$_3$ (Zhou et al., 2008), seemingly removing differential influences from halogen chemistry as the cause of year-to-year variability in Hg°.

Biomass burning can reportedly contribute to the ambient level of Hg° (e.g. Brunke et al., 2001; Friedli et al., 2001; Sigler and Lee, 2003). Data from Canada (http://nfdp.ccfm.org) shows that total area burned in Quebec and Ontario were much higher in 2005 than in 2004. In 2004, there was more precipitation and fewer hectares burned in Québec and Ontario, where we know there are fires that can influence the northeast US (Sigler and Lee, 2003; DeBell

et al., 2004). Hence, should emissions of biomass burning be the dominant effect, one would expect lower levels of Hg°, not higher, during the warm season in 2004 than in 2005. However, the steeper decreasing trend and the much lower annual minimum value in the 2005 warming season contradicts this piece of information. The US national data (http://www.nifc.gov/fire_info/fires_acres.htm) shows no significant difference in total burned area between 2004 and 2005 nationwide (and most of the burning takes place out west and, especially, in Alaska). Therefore, the impact of emissions from biomass burning was ruled out on the variation in Hg° levels from the warm season of 2004 to that of 2005.

Finally, a suite of climate variables was examined for the two year period, and no significant difference in atmospheric circulation patterns (e.g. sea level pressure, SLP), temperature, moisture, radiation flux, or wind speed/direction was identified. However, precipitation during the period of 1 April–30 September in 2004 was 173 mm more than over the same period in 2005. Documented effects of precipitation on Hg° levels are threefold: (1) a short-lived (∼hours) burst in emissions from soils usually occurs (Lindberg et al., 1999), (2) the dry deposition flux to a wet canopy can be enhanced up to 3-fold compared to a dry one (Lindberg et al., 1998) and, (3) reduced uptake/emission as forest stomatal exchange decreases strongly under dark conditions and drought stress (Lindberg et al., 1998). Recently, Bash and Miller (2008) found, based on flux measurements, that mercury evasion was greatest during periods when the canopy was wet from either dew or rainfall. This result suggests that depositional losses are more than offset by release of Hg° from the canopy, possibly due to lack of RGM which is more soluble than Hg°, or enhanced mobility and reduction of divalent mercury bound in soils or the canopy under wet conditions. It is possible that the dry conditions in summer 2005 may have contributed to the stronger decreasing trend that year. Measurements of RGM mixing ratios and both soil and canopy Hg° flux information are needed to conduct a robust assessment of these processes.

7.2 Wintertime Hg°

In contrast to the large year-to-year variability in the warm season Hg° levels, relatively small changes were observed in maximum Hg° levels from winters 2004 and 2005 to winters 2006 and 2007, when significant decreases in the maximum mixing ratios of CO, CO_2, NO_y, and SO_2 were captured by our measurements. The Hg° level varied slightly, while the maximum NO_y mixing ratio was lowered from 140 nmol/mol in 2004 and 2005 to 40 nmol/mol in 2006 and 2007 (Fig. 6) and CO from near 1000 nmol/mol to almost 400 nmol/mol (Fig. 5). This downward shift changed the relationship of Hg° with other trace gases via variation in the slope values of their linear correlations. Contributing factors to such changes can include fluctuations in anthropogenic emissions, climate,

and/or the chemical environment. The chemical processes affecting the five trace gases are different and complex, and it is difficult to obtain year-to-year mercury emission inventories. Therefore, we examined the dominant climate pattern of the four winters as the first step to understanding interannual variability in Hg°.

We found that the 2004–2007 winters in the northeastern US were characterized by a transition from cold to near normal conditions in 2004 and 2005 to significantly warmer than normal conditions in 2006 and 2007. Normal conditions are defined by the Northeast Regional Climate Center as the 30-year means over 1971–2000 (http://www.nrcc.cornell.edu/ /climate/Climate_summary.html). The average temperature in the northeastern US in 2004 was reportedly 1.1°C colder than normal while in 2005 it was near normal at just 0.2°C above the 30-year mean. In contrast, 2006 was 1.5°C warmer than normal and ranked as the 15th warmest winter on record since 1896, while 2007 was 1.0°C warmer than normal.

The spatial distribution of SLP in the northeastern US indicated that the cooler years of 2004 and 2005 were characterized by greater meridional flow, in stark contrast to more zonal flow in the warmer winters of 2006 and 2007 (Fig. 13). The greater meridional flow in 2004 and 2005 facilitated transport of colder air from the Polar Regions to the Northeast, which explains the colder climate in winters 2004 and 2005.

To understand the potential impact of such climate interannual variability on the redistribution of air pollutants, we examined the potential source regions corresponding to all the data points with $NO_y > 40$ nmol/mol, which indicate heavily polluted air masses, over the entire study time period at TF (1 December 2003–31 May 2007). There were 21 episodes during the four winters from the entire dataset (i.e. an episode is defined as a time period with continuous $NO_y > 40$ nmol/mol). Five-day backward trajectories were simulated using HYSPLIT (Draxler, 1999) every 5–6 h during each episode starting at altitudes of 500 m and 1000 m from TF, which yield 55 trajectories in total. Fifteen of the 55 trajectories stayed over the North American continent with the rest (40) originating from as far north as 60° N which followed the paths of either direct northerly flow, or northerly flow which traversed midwestern and southern states before veering northward along the eastern US and arriving at TF (Fig. 14). Thirteen of the 21 episodes occurred in winters 2004 and 2005 and only 8 in winters 2006 and 2007. This is consistent with the circulation patterns shown in Fig. 13, where the northerly flow on the front of the Canadian high and the back of the Labrador Low brought air masses from higher latitudes to the southeastern US before turning northward. Such flow regimes facilitate the transport Arctic air masses directly southward to midlatitudes accompanied by entrainment of pollutants from the densely populated eastern US.

Numerous studies indicate that wintertime Arctic air can be heavily polluted by long-range transport from Eurasia and
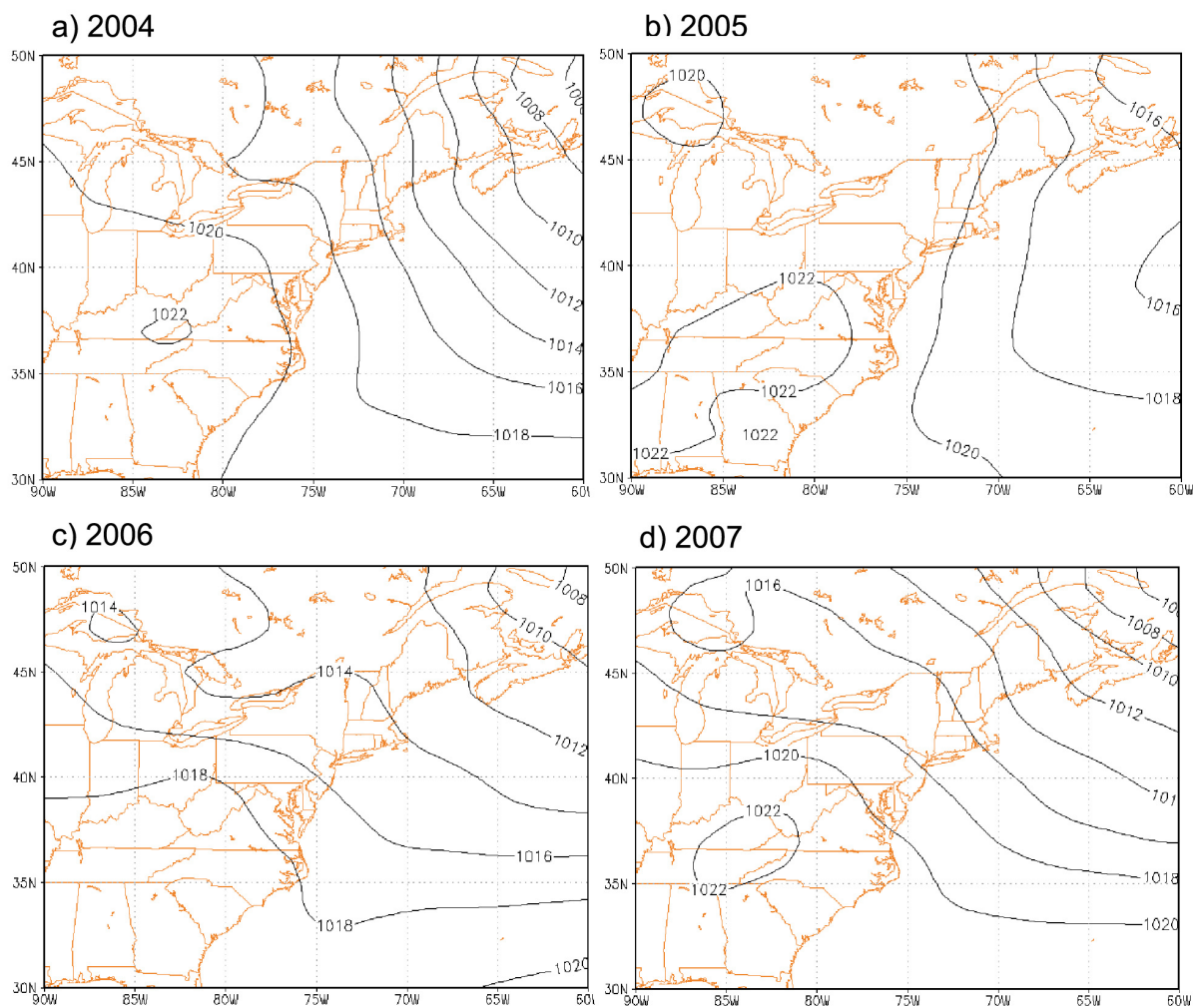
Fig. 13. Seasonally averaged sea level pressure for winters 2004 **(a)**, 2005 **(b)**, 2006 **(c)** and 2007 **(d)**.
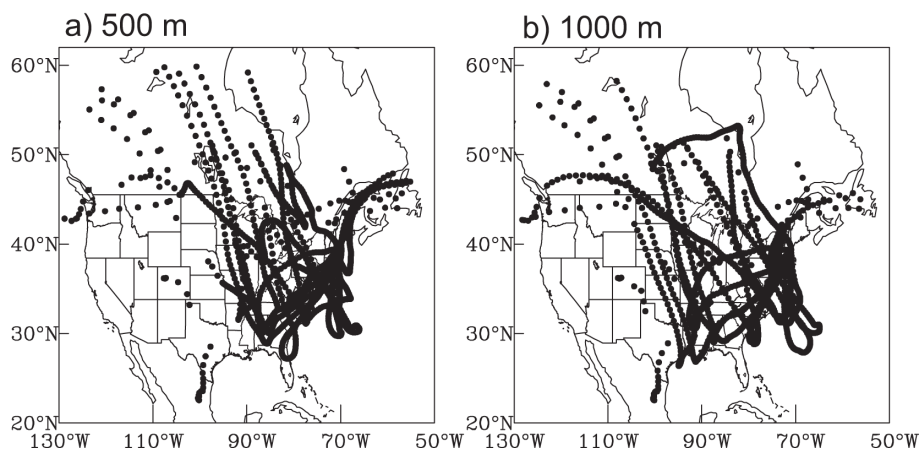

Fig. 14. Five-day backward trajectories using HYSPLIT for the 21 episodes of $NO_y > 40$ nmol/mol in winters 2004–2007 starting at two heights, 500 m **(a)** an 1000 m **(b)**, at TF.
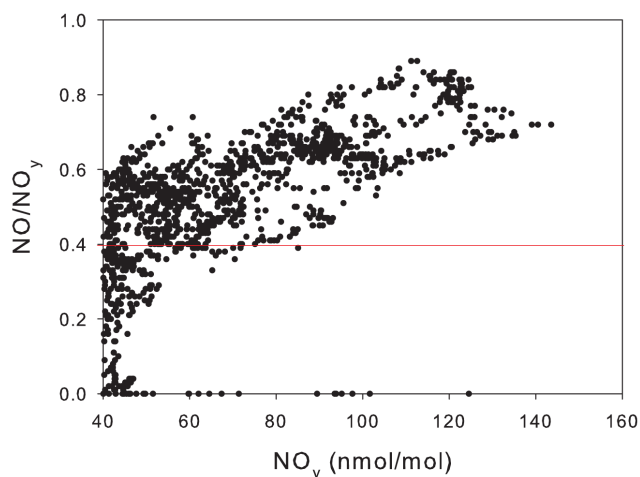
Fig. 15. Ratio of NO/NO$_y$ versus NO$_y$ at TF for all data points with NO$_y$ > 40 nmol/mol in winters 2004–2007.

North America (Wang et al., 2003; Stohl, 2006). Lamarque and Hess (2003) found that during the winter, CO in the lower troposphere at high latitudes was strongly influenced by fresh emissions from Europe, and also that aged emissions appeared to build up due to minimal photooxidation in the dark. Hence, it is reasonable to expect that Arctic air masses transported via meridional flow contribute to increased air pollutants at midlatitudes (Mao and Talbot, 2004c). However, such enhancements can easily be obscured by entrainment of fresh pollutants emitted in the eastern US. For instance, at TF there was a well-defined positive correlation between the NO$_y$ level > 40 nmol/mol and NO mixing ratios. For the majority data with NO$_y$ levels > 40 nmol/mol, NO comprised 40%–90% of NO$_y$ (Fig. 15). The lifetime of NO in the winter troposphere is ~1.5 days (Munger et al., 1998), and thus such high levels of NO most likely came from sources in the eastern US.

Surprisingly, mixing ratios of Hg° at TF rose only slightly during the 21 wintertime episodes. In the wintertime Arctic, Hg° concentration was found to be 1.84 ng m^{-3} (~200 fmol/mol) by Schroeder et al. (1998), or more than 20 fmol/mol higher than the seasonal median values of 160–180 fmol/mol at TF (Table 1). This suggests that Hg° at TF would be elevated, albeit perhaps not significantly, under the direct influence of Arctic air. Furthermore, it would be anticipated that the Arctic air mass in winters 2004 and 2005 should have entrained additional mercury during transport over the US. The observed small increases in Hg° under such circumstances implies: 1.) a homogeneous distribution of surface Hg° levels over the North American continent in winter, and/or 2.) a relatively smaller impact of the eastern US anthropogenic mercury emissions due to RGM comprising a significant portion of the total mercury emissions (e.g. ~34% of the total mercury emission from coal fire plants averaged in the US, Sullivan et al., 2006).

The second implication can also be used to explain the lower slope values in the two heavily polluted winters of 2004 and 2005, when changes in Hg° and CO should be dominated by their anthropogenic emissions. Emitted CO is mostly retained in the atmosphere during winter due to its long lifetime, while RGM is likely removed quickly after entering the atmosphere. Consequently, the ultimate anthropogenic contribution of mercury is likely smaller than that of CO, leading to smaller Hg°-CO slope values in those winters.

For the winters 2006 and 2007, the larger slope value in the Arctic air mass transported to TF directly from the north was most likely caused by two factors. First, there was minimal entrainment of fresh anthropogenic emissions. Second, decreases in Hg° due to loss of dry deposition and dilution with ambient air probably exceeded reductions in CO that would have occurred by dilution and minimal chemical loss. Therefore, we suggest that the wintertime Hg°-CO relationship should be used cautiously to estimate the anthropogenic contribution to ambient Hg°.

8 Summary

A comprehensive analysis was conducted using multiple years of Hg° measurements at two inland sites, TF and PM, and one summer of measurements at a marine site, AI, from the UNH AIRMAP observing network in southern New Hampshire. A large suite of other trace gases, e.g. CO, CO$_2$, CH$_4$, NO$_y$, NO, SO$_2$, and VOCs, were employed to identify possible sources of Hg° in New England. The measurements of Hg° at TF showed distinct seasonality with annual maxima in late winter – early spring and minima in early fall, with large day-to-day variation. A decreasing trend in the mixing ratio of Hg° over the time period of March–September occurred at a rate of 0.5–0.6 fmol/mol d^{-1} for all years except 2004 (0.3 fmol/mol d^{-1}). Measurements of Hg° at PM exhibited much smaller daily and annual variation, particularly reflected in the slower warm season decline (relative to TF) of 0.2 and 0.3 fmol/mol d^{-1} in 2005 and 2006, respectively. The AI data appeared to track the variation observed at TF albeit with much higher minima.

Hg° was correlated most strongly with CO and NO$_y$ in winter. The Hg°-CO relationship at PM suggested that the primary source of Hg° in winter is anthropogenic emissions. Applying the Hg°-CO relationship, we found that the seasonally averaged Hg° mixing ratio of ~160 fmol/mol at PM can be considered the regional background level. The positive Hg°-NO$_y$ correlation along the lower boundary of all data points indicated dry deposition as a stronger sink for Hg° than suggested by previous studies. We estimated a dry deposition velocity of 0.17–0.20 cm s^{-1} for Hg°, and a lifetime of ~16 days in the local boundary layer at TF.

It should be noted that a weak but positive correlation was found between Hg° and CHBr$_3$ at both TF and AI, which suggests a role of the oceanic source influencing the ambient

levels of Hg° in the marine and coastal environments. It was also hypothesized that the overall significantly lower Hg° levels and steeper decreasing trend during the warm season at TF compared to those at PM may reflect the impact of marine halogen chemistry.

Contrasting interannual variability in Hg° levels was identified between the warm and cold seasons. The stronger decline in warm season Hg° during 2005 and 2006 compared to 2004 may indicate that changes in precipitation played a role in mitigating evasion from the surface. In contrast, the Hg° level showed relative small changes from winters 2004 and 2005 to winters 2006 and 2007 while the mixing ratios of CO, CO_2, NO_y, and SO_2 decreased dramatically. Our measurements suggested that the predominant meridional flows in colder winters transported the polluted Arctic air mass across the US and then veered northward to TF while entraining fresh emissions, which resulted in high levels of anthropogenic tracers. However, little variation in Hg° possibly indicates a homogeneous distribution of surface Hg° in winter and/or rapid removal of RGM released from anthropogenic sources. During warmer winters the Hg°-CO slope value possibly reflects the ratio of Hg° loss relative to changes in CO more than their emission ratios.

Edited by: R. Sander

References

Ambrose, J. L., Mao, H., Mayne, H. R., Stutz, J., Talbot, R. W., and Sive, B. C.: Nighttime nitrate radical chemistry at Appledore Island, ME during ICARTT 2004, J. Geophys. Res., 112, D21302, doi:10.1029/2007JD008756, 2007.

Ariya, P. A., Khalizov, A., and Gidas, A.: Reactions of gaseous mercury with atomic and molecular halogens: kinetics, product studies, and atmospheric implications, J. Phys. Chem. A, 106, 7310–7320, 2002.

Bash, J. O. and Miller, D. R.: A relaxed eddy accumulation system for measuring surface fluxes of total gaseous mercury (TGM), J. Atmos. Oceanic Technol., 25(2), 244–257, doi:10.1175/2007JTECHA908.1, 2008.

Berg, T. and Aspmo, K.: Atmospheric mercury at the Zeppelin station, 889/2003, Norwegian Institute for Air Research, Statlig program for forurensnigsovervåking, NILU OR 86/2003, 2003.

Bergan, T., Gallardo, L., and Rodhe, H.: Mercury in the global troposphere: a three-dimensional model study, Atmos. Environ., 33, 1575–1585, 1999.

Brown, S. S., Dibb, J. E., Stark, H., et al.: Nighttime removal of NO_x in the summer marine boundary layer, Geophys. Res. Lett., 31, L07108, doi:10.1029/2004GLo19412, 2004.

Brunke, E., Labuschagne, C., and Slemr, F.: Gaseous mercury emissions from a fire in the Cape Peninsula, South Africa, during January 2000, Geophys. Res. Lett., 28(8), 1483–1486, 2001.

Calvert, J. G. and Lindberg, S. E.: Mechanisms of mercury removal by O_3 and OH in the atmosphere, Atmos. Environ., 39, 3355–3367, 2005.

Chen, M., Talbot, R., Mao, H., Sive, B., Chen, J., and Griffin, R. J.: Air mass classification in coastal New England and its relationship to meteorological conditions, J. Geophys. Res., 112, D10S05, doi:10.1029/2006JD007687, 2007.

DeBell, L. J., Talbot, R. W., Dibb, J. E., Munger, J. W., Fischer, E. V., and Frolking, S. E.: A major regional air pollution event in the northeastern United States caused by extensive forest fires in Quebec, Canada, J. Geophys. Res., 109, D19305, doi:10.1029/2004JD004840, 2004.

Dickerson, R. R., Rhoads, K. P., Carsey, T. P., Oltmans, S. J., Burrows, J. P., and Crutzen, P. J.: Ozone in the remote marine boundary layer: A possible role for halogens, J. Geophys. Res., 104(D17), 21 385–21 395, 1999.

Draxler, R. R.: HYSPLIT_4 (HYbrid Single-Particle Lagrangian Integrated Trajectory Version 4) User's Guide, NOAA Technical Memorandum ERL ARL-230, June 1999.

Fehsenfeld, F. C., Ancellet, G., and Bates, T. S., et al.: International Consortium for Atmospheric Research on Transport and Transformation (ICARTT): North America to Europe – Overview of the 2004 summer field study, J. Geophys. Res., 111, D23S01, doi:10.1029/2006JD007829, 2006.

Fischer, E., Pszenny, A., Keene, W., Maben, J., Smith, A., Stohl, A., and Talbot, R.: Nitric acid phase partitioning and cycling in the New England coastal atmosphere, J. Geophys. Res., 111, D23S09, doi:10.1029/2006JD007328, 2006.

Fischer, E. V., Ziemba, L. D., Talbot, R. W., Dibb, J. E., Griffin, R. J., Husain, L., and Grant, A. N.: Aerosol major ion record at Mount Washington, J. Geophys. Res., 112, D02303, doi:10.1029/2006JD007253, 2007.

Friedli, H. R., Radke, L. F., and Lu, J. Y.: Mercury in smoke from biomass fires, Geophys. Res. Lett., 28(17), 3223–3226, 2001.

Friedli, H. R., Tadke, L. F., Prescott, R., Li, P., Woo, J.-H., and Carmichael, G. R.: Mercury in the atmosphere around Japan, Korea, and China as observed during the 2001 ACE-Asia field campaign: Measurements, distributions, sources, and implications, J. Geophys. Res., 109, D19S25, doi:10.1029/2003JD004244, 2004.

Hall, B.: The gas phase oxidation of elemental mercury by ozone, Water, Air, Soil Pollution, 80(1–4), 301–315, doi:10.1007/BF01189680, 1995.

Hogrefe, C., Rao, S. T., Zurbenko, I. G., and Porter, P. S.: Interpreting the information in ozone observations and model predictions relevant to regulatory policies in the eastern United States, B. Am. Meteorol. Soc., 81, 2083–2106, 2000.

Jacob, D. J.: Introduction to atmospheric chemistry, Princeton University Press, Princeton, New Jersey, 25–26, 1999.

Kindler, T. P., Chameides, W. L., Wine, P. H., Cunnold, D. M., Alyea, F. N., and Franklin, J. A.: The fate of atmospheric phosgene and the stratospheric chlorine loadings of its parent compounds: CCl_4, C_2Cl_4, C_2HCl_3, CH_3CCl_3, and $CHCl_3$, J. Geophys. Res., 100(Dl), 1235–1251, 1995.

Kellerhals, M., Beauchamp, St., Belzer, W., et al.: Temporal and spatial variability of total gaseous mercury in Canada: results

from the Canadian Atmospheric Mercury Measurement Network (CAMNet), Atmos. Environ., 37, 1003–1011, 2003.

Kim, K.-H., Ebinghaus, R., and Schroeder, W. H., et al.: Atmospheric mercury concentrations from several observatory sites in the Northern Hemisphere, J. Atmos. Chem., 50, 1–24, 2005.

Lamarque, J.-F. and Hess, P. G.: Model analysis of the temporal and geographical origin of the CO distribution during the TOPSE campaign, J. Geophys. Res., 108(D4), 8354, doi:10.1029/2002JD002077, 2003.

Laurier, F. J. G., Mason, R. P., and Whalin, L.: Reactive gaseous mercury formation in the North Pacific Ocean's marine boundary layer: A potential role of halogen chemistry, J. Geophys. Res., 108(D17), 4529, doi:10.1029/2003JD003625, 2003.

Laurier, F. and Mason, R.: Mercury concentration and speciation in the coastal and open ocean boundary layer, J. Geophys. Res., 112, D06302, doi:10.1029/2006JD007320, 2007.

Lee, D. S., Dollard, G. J., and Pepler, S.: Gas phase mercury in the atmosphere of the United Kingdom, Atmos. Environ., 32, 855–864, 1998.

Lee, D. S., Nemitz, E., Fowler, D., and Kingdon, R. D.: Modeling atmospheric mercury transport and deposition across Europe and the UK, Atmos. Environ., 35, 5455–5466, 2001.

Lin, C.-J., Pongprueksa, P., Lindberg, S. E., Pehkonen, S. O., Byun, D., and Jang, C.: Scientific uncertainties in atmospheric mercury models I: Model science evaluation, Atmos. Environ., 40, 2911–2928, 2006.

Lindberg, S. E., Meyers, T. P., Taylor, G. E., Turner, R. R., and Schroeder, W. H.: Atmosphere-surface exchange of mercury in a forest: Results of modeling and gradient approaches, J. Geophys. Res., 97, 2519–2528, 1992.

Lindberg, S. E. and Stratton, W. J.: Atmospheric mercury speciation: concentrations and behavior of reactive gaseous mercury in ambient air, Environ. Sci. Technol., 32(1), 49–57, 1998.

Lindberg, S. E., Hanson, P. J., Meyers, T. P., and Kim, K.-H.: Air/surface exchange of mercury vapor over forests – The need for a reassessment of continental biogenic emissions, Atmos. Environ., 32(5), 895–908, 1998.

Lindberg, S. E., Zang, H., and Gustin, M., et al.: Increases in mercury emission from desert soils in response to rainfall and irrigation, J. Geophys. Res., 104(D17), 21 879–21 888, 1999.

Mao, H. and Talbot, R.: O$_3$ and CO in New England: Temporal variations and relationships, J. Geophys. Res., 109, D21304, doi:10.1029/2004JD004913, 2004a.

Mao, H. and Talbot, R.: Role of meteorological processes in two New England ozone episodes during summer 2001, J. Geophys. Res., 109, D20305, doi:10.1029/2004JD004850, 2004b.

Mao, H. and Talbot, R.: Relationship of surface O$_3$ to large-scale circulation patterns during two recent winters, Geophys. Res. Lett., 31, L06108, doi:10.1029/2003GL018860, 2004c.

Mason, R. P. and Sheu, G.-R.: Role of the ocean in the global mercury cycle, Global Biochem. Cycles, 16(4), 1093, doi:10.1029/2001GB001440, 2002.

Miller, S. T. K., Keim, B. D., Talbot, R. W., and Mao, H.: Sea breeze: Structure, forecasting, and impacts, Rev. Geophys., 41(3), 1011, doi:10.1029/2003RG000124, 2003.

Munger, J. W., Fan, S. M., Bakwin, P. S., Goulden, M. L., Goldstein, A. H., Colman, A. S., and Wofsy, S. C.: Regional budgets for nitrogen oxides from continental sources: Variations of rates for oxidation and deposition with season and distance from source

regions, J. Geophys. Res., 103, 8355–8368, 1998.

NESCAUM: Economic Valuation of Human Health Benefits of Controlling Mercury Emissions from U.S. Coal-Fired Power Plants, Northeast States for Coordinated Air Use Management, Boston, MA, 2005a.

NESCAUM: Inventory of Anthropogenic Mercury Emissions in the Northeast, Northeast States for Coordinated Air Use Management, Boston, MA, 2005b.

NOAA GMD: Annual Report #26, http://www.esrl.noaa.gov/gmd/publications/annrpt26/, 2000.

Obrist, D., Conen, F., Vogt, R., Siegwolf, R., and Alewell, C.: Estimation of Hg° exchange between ecosystems and the atmosphere using ^{222}Rn and Hg° concentration changes in the stable nocturnal boundary layer, Atmos. Environ., 40, 856–866, 2006.

Olaguer, E. P.: The distribution of the chlorinated solvents dichloromethane, perchloroethylene, and trichloroethylene in the global atmosphere, Environ. Sci. Pollut. Res., 9, 175–182, 2002.

Pai, P., Karamchandani, P., Seigneur, C., and Allan, M.: Sensitivity of simulated atmospheric mercury concentrations and deposition to model input parameters, Atmos. Environ., 31, 2717–2732, 1997.

Pacyna, E. G. and Pacyna, J. M.: Global emission of mercury from anthropogenic sources in 1995, Water, Air, Soil Pollut., 137, 149–165, 2002.

Parrish, D. D., Holloway, J. S., Trainer, M., Murphy, P. C., Forbes, G. L., and Fehsenfeld, F. C.: Export of North American ozone pollution to the North Atlantic Ocean, Science, 259, 1436–1439, 1993.

Poissant, L., Pilote, M., Xu, X., Zhang, H., and Beauvais, C.: Atmospheric mercury speciation and deposition in the Bay of St. Francois wetlands, J. Geophys. Res., 109, D11301, doi:10.1029/2003JD004364, 2004.

Poissant, L., Pilote, M., Constant, P., Beauvais, C., and Zhang, H. H.: A year of continuous measurements of three atmospheric mercury species (GEM, RGM, and Hg$_p$) in southern Québec, Canada, Atmos. Environ., 39, 1275–1287, 2005.

Schroeder, W. H. and Munthe, J.: Atmospheric mercury – an overview, Atmos. Environ., 5, 809–822, 1998.

Seigneur, C., Vijayaraghavan, K., Lohman, K., Karamchandani, P., and Scott, C.: Global source attribution for mercury deposition in the United States, Environ. Sci. Technol. 38, 555–569, 2004.

Sheu, G.-R.: Speciation and distribution of atmospheric mercury: Significance of reactive gaseous mercury in the global mercury cycle, Ph.D. Thesis, University of Maryland, College Park, pp. 170, 2001.

Shipham, M. C., Bartlett, K. B., Crill, P. M., Harriss, R. C., and Blaha, D.: Atmospheric methane measurements in central New England: An analysis of the long-term trend and the seasonal and diurnal cycles, J. Geophys. Res., 103(D9), 10 621–10 630, 1998a.

Shipham, M. C., Crill, P. M., Bartlett, K. B., Goldstein, A. H., Czepiel, P. M., Harriss, R. C., and Blaha, D.: Methane measurements in central New England: An assessment of regional transport from surrounding sources, J. Geophys. Res., 103, 21 985–22 000, 1998b.

Sigler, J. M., Lee, X.-H., and Munger, J. W.: Emission and long-range transport of mercury from a Canadian boreal forest fire, Environ. Sci. Technol. 37(19), 4343–4347, 2003.

Sigler, J. M. and Lee, X.-H.: Gaseous mercury in background for-

est soil in the northeastern United States, J. Geophys. Res., 111, G02007, doi:10.1029/2005JG000106, 2006.

Sive, B. C., Zhou, Y., Troop, D., Wang, Y., Little, W. C., Wingenter, O. W., Russo, R. S., Varner, R. K., and Talbot, R.: Development of a cryogen-free concentration system for measurements of volatile organic compounds, Anal. Chem., 77(21), 6989–6998, doi:10.1021/ac0506231, 2005.

Sommar, J., Gårdfeld, K., Strömberg, D., and Feng, X.: A kinetic study of the gas-phase reaction between the hydroxyl radical and atomic mercury, Atmos. Environ., 35, 3049–3054, 2001.

Sommar, J., Hallquist, M., Ljungström, E., and Lindqvist, O.: On the gas phase reactions between volatile biogenic mercury species and the nitrate radical, J. Atmos. Chem., 27, 233–247, 1997.

Spivakovsky, C. M., Logan, J. A., Montzka, S. A., et al.: Three-dimensional climatological distribution of tropospheric OH: Update and evaluation, J. Geophys. Res., 105(D7), 8931–8980, 2000.

Sprovieri, F., Pirrone, N., and Sommar, J.: Mercury speciation in the marine boundary layer along a 6000 km cruise path around the Mediterranean Sea, Atmos. Environ., 37, suppl. 1, S63–S71, 2003.

Stohl, A.: Characteristics of atmospheric transport into the Arctic troposphere, J. Geophys. Res., 111, D11306, doi:10.1029/2005JD006888, 2006.

Sullivan, T. M., Adams, J., Milian, L., Subramaniam, S., Feagin, L., Williams, J., and Boyd, A.: Local impacts of mercury emissions from the Monticellow coal fired power plant, BNL-77475-2007-IR, Environmental Sciences Department, Environmental Research & Technology Division, Brookhaven National Laboratory, P.O. Box 5000, Upton, NY 11973-5000, 2006.

Talbot, R., Mao, H., and Sive, B.: Diurnal characteristics of surface level O_3 and other important trace gases in New England, J. Geophys. Res., 110, D09307, doi:10.1029/2004JD005449, 2005.

Talbot, R. W., Brown, D., Bryce, J., Chen, M., Griffin, R., McDowell, W., Mao, H., Mayne, H., Sive, B., Varner, R., Wake, C., Koermer, J., and Pszenny, A.: AIRMAP: A UNH Air Quality and Climate Program, Semi-Annual Technical Report to Office of Oceanic and Atmospheric Research and NOAA Earth Systems Research Laboratory, National Oceanic and Atmospheric Administration, Silver Spring, MD, 57 pp., December 2006.

Valente, R. J., Shea, C., Humes, K. L., and Tanner, R. L.: Atmospheric mercury in the Great Smoky Mountains compared to regional and global levels, Atmos. Environ., 41, 1861–1873, 2007.

Wang, Y., Shim, C., Blake, N., et al.: Intercontinental transport of pollution manifested in the variability and seasonal trend of springtime O_3 at northern middle and high latitudes, J. Geophys. Res., 108, 4683, doi:10.1029/2003JD003592, 2003.

Xu, X., Yang, X., Miller, D., Helble, J. J., and Carley, R. J.: Formulation of bi-directional atmosphere-surface exchanges of elemental mercury, Atmos. Environ., 33, 4345–4355, 1999.

Zhou, Y., Varner, R. K., Russo, R. S., Wingenter, O. W., Haase, K. B., Talbot, R., and Sive, B. C.: Coastal water source of short-lived halocarbons in New England, J. Geophys. Res., 110, D21302, doi:10.1029/2004JD005603, 2005.

Zhou, Y., Varner, R. K., Mao, H., Russo, R. S., Blake, D. R., Wingenter, O. W., Haase, K. B., Talbot, R., and Sive, B. C.: Bromoform and dibromomethane measurements in the seacoast region of New Hampshire, 2002–2004, J. Geophys. Res., in press, 2008.

Zurbenko, I. G.: The Spectral Analysis of Time Series, North-Holland, 248 pp., 1986.